Amphibole Pairs, Epidote Minerals, Chlorite, and Plagioclase in Metamorphic Rocks, Northern Sierra Nevada, California[1]

ANNA HIETANEN

U. S. Geological Survey, Menlo Park, California

Electron microprobe analyses by G. K. CZAMANSKE

AREA
CA
Butte
Sierra

Abstract

Two kinds of amphiboles—actinolite and aluminous Ca-amphibole—and two to three epidote minerals coexist with chlorite and plagioclase in the meta-volcanic and meta-igneous rocks in the contact aureoles of the Cretaceous plutons in the Feather River area, northern Sierra Nevada. Small prisms and rims of actinolite occur with green hornblende outside the 1-mile-wide contact aureoles of the plutons. In the zone next to the plutons, blue-green hornblende forms rims around large grains of actinolite and also forms small prisms that are included in plagioclase. Electron-microprobe analyses show that the alkali and Al content of the amphiboles increases with an increase in the grade of metamorphism, the ratio of $Na+K$ to tetrahedral Al remaining close to 1:3. The ratio between two coupled substitutions, edenitic ($Na^A Al^{iv}$ for $\square^A Si^{iv}$) and tschermakitic ($Al^{vi} Al^{iv}$ for $Mg^{vi} Si^{iv}$), remains 3:7 and leads to the composition $Na_{0.3}Ca_2Mg_{2.4}Fe^{2+}_{1.0}(Al,Fe^{3+})_{1.3}Si_{6.3}Al_{1.7})O_{22}(OH)_2$ at the highest grade of metamorphism in the Feather River area and further to $Na_{0.6}Ca_2R^{2+}_{3.6}R^{3+}_{1.4}Si_6Al_2O_{22}(OH)_2$, the extreme member of this actinolite-hornblende series. The Mg/Fe ratio changes with the bulk composition and with the degree of oxidation of the host rocks. Epidote and clinozoisite coexist in all zones as separate grains. In addition, many grains of clinozoisite include high index domains, lamellae, and stringers of epidote. In the highest grade zone next to the plutons, zoisite occurs with epidote, clinozoisite, and anorthitic plagioclase. Farther from the plutons, the plagioclase is albite. There is no regular change in the distribution coefficient $K_D(Mg/Fe)$ for chlorite/amphibole although it is highest in the zone next to the plutons.

Introduction

The minerals studied occur as major constituents in Paleozoic(?) metavolcanic and related metamorphosed intrusive rocks around Cretaceous plutons in the southwestern part of the Bucks Lake quadrangle, northern Sierra Nevada. The general geology of this quadrangle and the petrography and chemical composition of the host rocks have been described in another report (Hietanen, 1973); therefore only a short summary of the geologic setting and some additional features are given in the following description.

Two metamorphic events can be recognized in the host rocks near the plutons. The earlier regional metamorphism was to the greenschist facies and was modified by a later higher-temperature contact metamorphism that affected only the rocks in a narrow zone around the plutons. In the pelitic layers, the common occurrence of andalusite, cordierite, and staurolite in the outer contact aureole and andalusite and cordierite in the inner one indicates *PT* conditions of the epidote amphibolite facies (Hietanen, 1967). Elsewhere, mineral assemblages such as muscovite-biotite-chlorite in pelitic layers and albite-epidote-actinolite-hornblende indicate the upper limit of the greenschist facies.

In the metavolcanic rocks and related intrusive rocks, the increase in the grade of metamorphism is indicated by the change of the color of hornblende. In the low-grade zone, the pleochroism parallel to γ is light green to green but becomes bluish green towards the plutons. The most interesting feature is that two amphiboles—actinolite and aluminous hornblende—and two to three epidote minerals coexist in all zones, as shown by indices of refraction measured in immersion liquids. It was therefore highly desirable to determine the composition of these coexisting minerals. The rock samples chosen

for this study had already been chemically analyzed (Hietanen, 1973, Table 1). They include intermediate and basic metavolcanic rocks and related intrusive rocks, metadiorites, and metagabbros.

Samples of meta-andesite and metadacite (samples 463 and 464) are from successive layers in the Franklin Canyon Formation, 3.2 miles east-southeast of the Granite Basin pluton (Fig. 1). Sample 465 is from a small body of metadiorite a few meters wide just south of the locality of metadacite sample 464. Because of their proximity, these three rocks most likely recrystallized at the same PT conditions at the border of the greenschist and epidote amphibolite facies. The four other samples (Sp. 796, 546, 551, 532) were collected from 0.3 to 0.8 mile outside the contact of the Granite Basin pluton. The rocks in this contact zone are coarser grained and show a higher grade of metamorphism than those farther from the contact.

Description of the Rocks

Metagabbro sample 796, 0.3 mile south of the Granite Basin pluton, represents the highest metamorphic grade. It is a coarse-grained dark rock in which black hornblende contrasts with white anorthite (An_{93}). Thin sections show that most of the large amphibole grains are pale-green to colorless actinolite ($\gamma \wedge c = 20°$) mottled with blue-green amphibole (Fig. 2). All large grains are rimmed by blue-green amphibole that is strongly pleochroic in blue green (γ), green (β), and light green (α) and has $\gamma \wedge c = 22°$. In addition, small euhedral prisms of blue-green amphibole are included in anorthitic plagioclase. Most plagioclase grains are granulated, individual grains averaging 0.01 mm in size, but some are large and have mottled extinction and irregular twinning lamellae. Some of these lamellae consist of rows of tiny small grains; others have wavy borders similar to those described in an earlier report
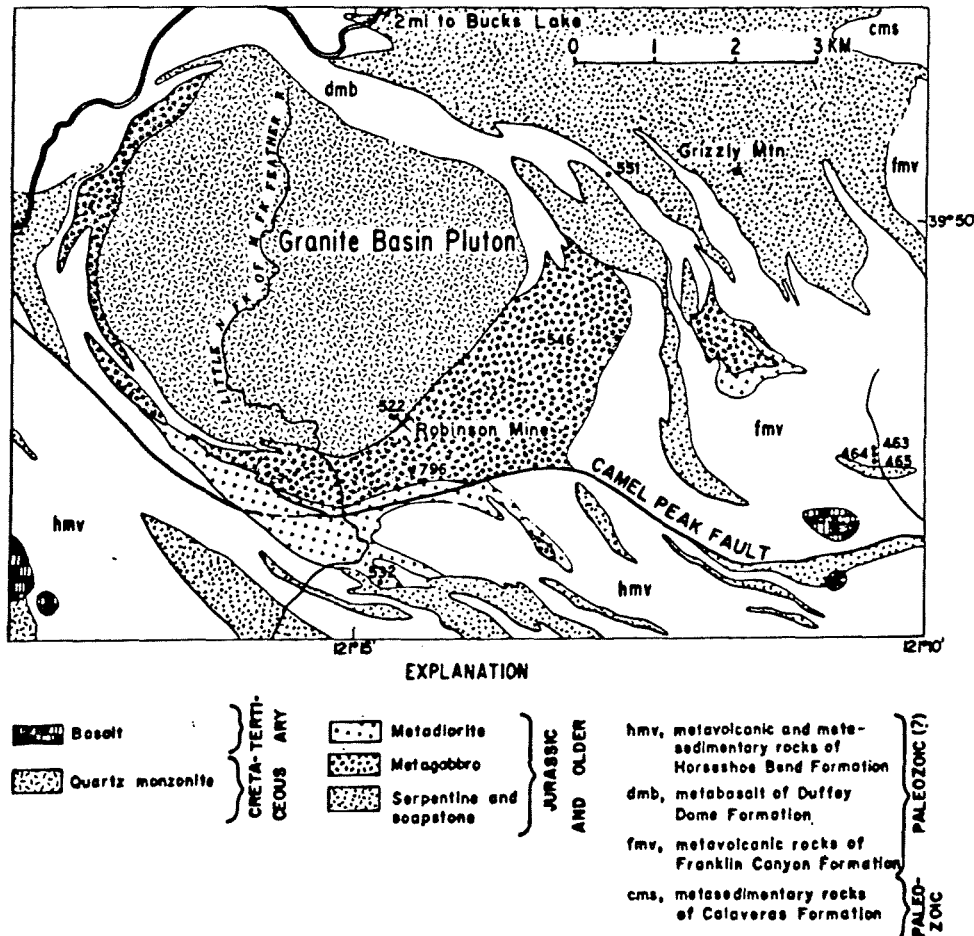

EXPLANATION

FIG. 1. Major geologic units and locations of the specimens studied (796, 546, 463, 532 and 464) in the Feather River area.
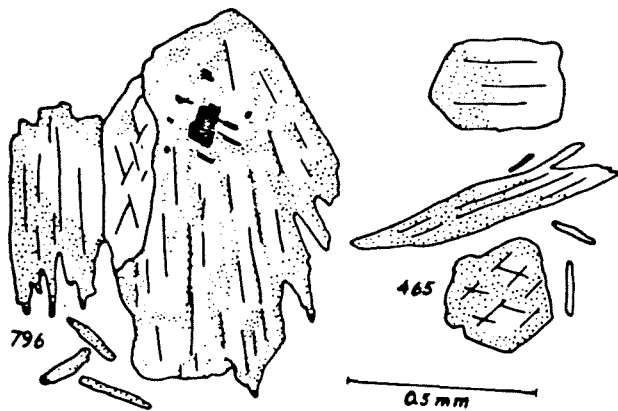
FIG. 2. Amphibole grains consisting of hornblende (shaded) and actinolite (unshaded). Black is magnetite. In the high grade zone (796) actinolite has rims and patches of blue green hornblende, and small prisms of hornblende are included in anorthitic plagioclase. In the low grade zone (465) large grains consist either of actinolite with patches of green hornblende, or of hornblende that includes and is rimmed by actinolite. Small prisms of actinolite are included in albite.

(Hietanen, 1951, Fig. 21) and are thought to have crystallized from zoisite at elevated temperatures near the plutons. All three epidote minerals, epidote, clinozoisite, and iron-poor zoisite, are present. Epidote and clinozoisite are in individual grains or in clusters, which are surrounded by a mass of small grains of zoisite dusted with tiny inclusions (Fig. 3). Some clinozoisite grains contain patches of epidote; some others have twinning lamellae. All epidote minerals contain inclusions of leucoxene, and are accompanied by some chlorite and quartz. A few tiny grains of ilmenite-magnetite occur as an accessory.

Metagabbro sample 546, 0.4 mile east of the Granite Basin pluton, is mineralogically and texturally similar to the metagabbro of locality 796, except for the absence of zoisite, a lower anorthite content (An₇₀) in plagioclase, and less actinolite. A few blue-green hornblende prisms have actinolite ends.

Metabasalt sample 551, 0.8 mile east-northeast of the Granite Basin pluton, is a dark-green to black, weakly foliated rock that consists mainly of small prisms of hornblende, opaque minerals, and albitic plagioclase. In thin sections, hornblende prisms (0.2 to 1 mm long) are pleochroic in light blue-green and light green and have colorless actinolite ends or, more rarely, are partly rimmed by actinolite. They are subparallel to the foliation or form radiating clusters. Small very light green to colorless needles of actinolite occur next to the green hornblende and are

included in albite. Albite is in granulated grains among the hornblende prisms and includes small grains and clusters of epidote and some clinozoisite. Numerous scattered anhedral to subhedral grains of ilmenite (about 0.02 mm long) are included in hornblende; some larger ore grains are clustered parallel to the foliation. Some leucoxene is included in hornblende and epidote minerals.

Meta-andesite sample 463, 3.2 miles east-southeast of the Granite Basin pluton, is a fine-grained gray-green dense rock that is either massive or weakly foliated. Major constituents are light-green to pale-green hornblende, colorless actinolite, epidote, clinozoisite, and albite. Small amounts of chlorite, leucoxene, magnetite, and pyrrhotite are ubiquitous. The minerals are clustered; aggregates consisting of amphiboles and some chlorite and epidote minerals probably were originally pyroxene phenocrysts. In the massive rock, green hornblende occurs in anhedral to subhedral grains, 0.01 mm to 1 mm long. Many grains have pale-green to colorless actinolitic ends and rims; all contain inclusions of leucoxene. Actinolite also occurs as needles in albite. Albite is in small (0.1 to 0.3 mm) grains embedded in a mixture of small anhedral grains of epidote and clinozoisite that is clouded by leucoxene. In some small patches, however, euhedral crystals of epidote minerals free of inclusions are included in albite or in a mixture of albite, fine-grained epidote, and leucoxene. Chlorite is in clusters of small flakes next to the amphiboles in the massive rock and with epidote minerals along the foliated shear zones. The opaque minerals, pyrrhotite and magnetite, are in subhedral grains, 0.01 to 0.5 mm in size.

Metadiorite sample 465, which is considered to be an intrusive equivalent of the meta-andesite and metadacite, is an equigranular rock in which dark-green hornblende crystals contrast with the white to
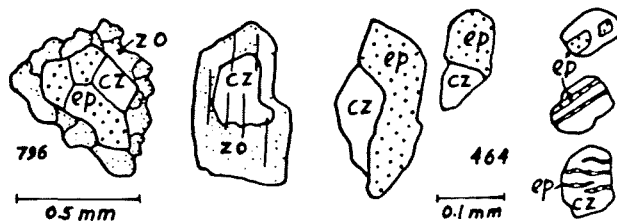

FIG. 3. Textural relations between epidote minerals from the high grade zone (796) and the low grade zone (464). ep = epidote, cz = clinozoisite, zo = zoisite. Domains, lamellae, and stringers of epidote in clinozoisite (far right) are textures seen in immersed fragments. The other grains are sketched from thin sections.

pale green mixture of albite and epidote minerals. Amphibole is in subhedral to euhedral prisms, 0.2 to 1 mm long, that are pleochroic in light to medium green; many prisms have pale green to colorless spots and ends (Fig. 2). Albite and epidote minerals form clusters that have outlines of former plagioclase, or they occur as small interstitial grains between these clusters and the hornblende prisms. Some of the epidote minerals are in large (0.5 mm long) crystals. Quartz is in small (0.01 to 0.5 mm long) grains or groups of grains among the other minerals. In places, clusters of very pale green chlorite flakes with brownish gray interference color occur between the amphibole and epidote minerals. Sphene is in anhedral grains adjacent to epidote or hornblende. Most of the original magnetite is altered to hematite.

In the metadiorite sample 532, 1 mile south of the Granite Basin pluton, anhedral grains (0.5 to 1 mm long) of green amphibole are embedded in a mixture consisting of albite and epidote. The amphibole is pleochroic in light bluish green to pale green and includes leucoxene. Albite grains are subhedral, 0.2 to 0.5 mm long, and include numerous small subhedral to anhedral crystals of epidote, some of which are clustered. A few patches, 0.5 mm long, consisting of tiny flakes of chlorite, occur next to amphibole grains. Magnetite is partly altered to hematite, and sphene to leucoxene.

Sample 532 is from the southeastern end of an elongate body that was emplaced along a fault zone (Camel Peak fault in Fig. 1). The major part of the body consists of light-colored porphyritic metatrondhjemite that contains about 35 percent quartz, 25 percent albite, 18 percent epidote and clinozoisite, 15 percent hornblende, and 7 percent chlorite. Small grains of ilmenite-magnetite are enveloped by sphene. Hornblende prisms have pleochroism γ = light blue-green, β = light green, α = pale green. Only a few small prisms of actinolite occur with green hornblende. Most of the clinozoisite is in long prisms among round grains of quartz that fill the fractures in the rock. Some slender needles, however, are included in albite. Thus metatrondhjemite in the main part of this metamorphosed intrusive body has two amphiboles and two epidote minerals, as do the other specimens studied. The occurrence of only a green hornblende and an epidote in the metadiorite (Sp. 532) indicates physical conditions different from those elsewhere during the recrystallization of this rock; perhaps this metadiorite is a later dike-like body in which epidote is late magmatic, comparable

with the epidote in the Jurassic plutons. It is also possible that there is a submicroscopic intergrowth of two phases in each mineral.

Metadacite sample 464 is a light-grayish-green inhomogeneous slightly foliated rock, in which dark patches, 1 to 20 mm long and consisting of chlorite, amphibole, clinozoisite, and epidote, are in the matrix of albite, quartz, chlorite, and epidote minerals. Amphibole is in small colorless to pale-green prisms that have ragged ends. Chlorite, the major dark constituent, is colorless, has a gray to brownish gray interference color and negative elongation, and includes tiny grains of leucoxene along its cleavage planes. Albite is in clusters of equant, subhedral grains that include epidote minerals and some small prisms of amphibole. Clinozoisite, the major epidote mineral, is clustered either with chlorite or with albite. Some clusters show the outlines of former pyroxene or former plagioclase. Epidote occurs either as individual grains or with clinozoisite (Fig. 3). The opaque minerals, pyrrhotite and magnetite, are in anhedral grains 0.2 and 0.5 mm in size. Albite is twinned and includes epidote minerals, chlorite, and some muscovite.

All these rocks are exceptionally poor in potassium (Hietanen, 1973, Table 1); K_2O content ranges from 0.03 to 0.21 percent.

The question about the possibility of equilibrium between the coexisting amphiboles and epidote minerals has to be considered in the light of thermal history of the host rocks. There were two periods of metamorphism: (1) low-grade regional metamorphism during which albite, epidote, actinolite, chlorite, and quartz crystallized from plagioclase, pyroxene, "igneous" hornblende, and biotite with or without quartz (the recrystallization may have not been complete); (2) later contact metamorphism at higher temperatures gave rise to crystallization of hornblende, clinozoisite, and zoisite at temperatures where epidote, actinolite, and chlorite were still stable. The absence of relict primary igneous minerals and chemical changes in bulk composition indicate a thorough reconstitution of rocks.

Textural relations in the high-grade zone (Sp. 796) suggest that the rims of blue-green hornblende around actinolite may have prevented further reaction between the actinolite cores and the plagioclase in the matrix. However, the occurrence of blue-green hornblende in patches in the centers of actinolite with its absence in parts of the rims refutes this concept and shows that a low rate of diffusion

of Al and Na was not the reason for preservation of actinolite cores. The high anorthite content of plagioclase (An_{93}) suggests that lack of available Na was one of the determining factors, but not the only one because the composition of blue-green hornblende + actinolite could give green hornblende with less Na. The occurrence of blue-green hornblende only in the high grade zone shows that it crystallized at elevated temperatures from bulk compositions similar to those that in the low grade zone produced green hornblende, albite, and actinolite. In parts of the metagabbro, as in sample 546, very little actinolite remains and plagioclase is An_{70}. This sample, collected a little farther from the contact of the pluton than sample 796, is thus from a somewhat lower temperature zone. Although considerable amount of sodium remains in the plagioclase, a few blue-green hornblende prisms in sample 546 have actinolite ends. The actinolite ends and rims are more common and remnants of the cores more rare farther from the pluton (Sp. 551). These ends and rims crystallized last, probably after the maximum metamorphic temperature was passed.

The textural relations between epidote and clinozoisite (Fig. 3) suggest that they coexist in equilibrium. Clinozoisite is in anhedral or in euhedral to subhedral crystals next to or among the anhedral epidote grains. Lamellae, stringers, and domains of epidote in clinozoisite resemble textures due to exsolution. Zoisite occurs only in the highest grade zone; it rims grains and clusters of epidote and clinozoisite and is thus later. The abundant dust-like inclusions in it are probably iron oxide exsolved when zoisite crystallized from epidote.

Optical Properties of Minerals

In the highest grade zone (Sp. 796) the blue-green hornblende is strongly pleochroic; farther from the pluton (Sp. 551) the colors are much lighter, and green hornblende in the low-grade zone has $\gamma =$ light green, $\beta =$ light green to olive green, and $\alpha =$ pale green. Actinolite in all specimens has $\gamma =$ pale green and β and α from very pale green to colorless. Many amphibole grains in samples 463, 464, and 465 have green centers and colorless rims. The contact between the center and the rim is usually diffuse. Many grains show intergrowths either of fine lamellae or of equant to elongate domains of green amphibole in colorless actinolite, all the green amphibole showing higher indices of refraction. Each amphibole has remarkably uniform indices of refraction

(Table 1) in all the rock types except in metabasalt sample 551, where they are somewhat higher; $\gamma \wedge c$ is generally 21° to 26° for the hornblende and about 15° for the actinolite.

The indices of refraction of amphibole grains (Table 1) can be correlated only in a general way with the microprobe analyses that were done in polished thin sections. The highest indices measured for actinolite are in sample 551, in which Fe/Mg ratio is higher than in the other specimens (Hietanen, 1973). Also the hornblende in this rock has higher indices of refraction than the hornblende in the other specimens apparently due to a high iron content (see Table 2a). High aluminum content, such as that in the blue-green hornblende in sample 796, affects indices of refraction far less than high Fe content. Specimens 463 and 465 also contain grains of actinolite similar to those in specimen 796. Only one amphibole, the green hornblende, was detected in the mineral powder from sample 532.

The epidote concentrate of the powdered rocks revealed two epidote minerals in all the samples, except in metadiorite sample 532 and in sample 796, which have one and three epidote minerals respectively. Many grains appeared to consist of small domains of epidote (with indices of refraction higher than 1.72) in clinozoisite (indices lower than 1.72). The high index domains range from lamellae parallel

TABLE 1. Indices of Refraction of Amphiboles, Epidote Minerals, and Chlorite

Sample Rock		796 Meta- gabbro	551 Meta- basalt	532 Meta- diorite	465 Meta- diorite	463 Meta- andesite	464 Meta- dacite
Hornblende	α	1.651	1.655	1.651	1.647	1.649	1.647
	β	1.659	1.669	1.659	1.658	1.657	
	γ	1.671	1.679	1.671	1.671	1.670	1.671
	γ∧c	22°	25°	24°	25°	21°	
Actinolite	α	1.625	1.640		1.625	1.626	1.622
	β	1.634	1.648				
	γ	1.648	1.666		1.649	1.650	1.647
Epidote	α	1.719	1.721	1.721	1.721	1.723	1.722
	β	1.732	1.731	1.733	1.741	1.743	
	γ	1.744	1.742	1.742 to 1.754	1.751	1.755	1.755
Clinozoisite	α	1.708	1.709		1.714	1.715	1.709
	β	1.710	1.711		1.716	1.717	
	γ	1.718	1.720		1.722	1.722	1.721
Zoisite	α	1.699					
	β	1.703					
	γ	1.714					
Chlorite	γ	1.600		1.620	1.615	1.617	
	+2V	~10°		small	small	small	small
Muscovite	β	1.591					
	γ	1.593					
Plagioclase	α	1.574		1.530		1.530	1.529
	β	1.581		1.534		1.533	1.533
	γ	1.585		1.539		1.538	1.538

to the cleavage and perthitelike intergrowths to small equant domains of epidote in clinozoisite, all of which still show ultrablue interference color (Fig. 3, at right). The contacts between the domains and the host mineral seem sharp.

The measurements in the individual samples (Table 1) show that the indices of refraction of epidote and clinozoisite in the samples from the low grade zone tend to be higher than those from the high grade zone. In all the epidotes $2V_x$ is large. In addition to clinozoisite and epidote, zoisite with gray interference colors, parallel extinction, $2V_z \sim 50°$, and indices of refraction lower than those of clinozoisite occurs in metagabbro (sample 796). The highest γ measured is given for clinozoisite in Table 1. This value is higher than would be expected on basis of a large $+2V$ and is due to a range in composition.

Chlorite occurs in clusters of small flakes in all rocks. It is most abundant in metadacite sample 464 and occurs only sporadically in metagabbro sample 796. It is pleochroic $\gamma = \beta =$ green, $\alpha =$ colorless in samples 796, 551, and 532, but very pale green to colorless in the other samples. The indices of refraction of the green chlorite in sample 532 are somewhat higher, and those in sample 796 are lower than the indices of the common pale variety (Table 1). All chlorites have brownish gray interference color, negative elongation, and small $+2V$.

The indices of refraction of plagioclase (Table 1) indicate that it is albite in the low grade zone and anorthite at the highest grade next to the pluton.

Composition of Minerals

Separation of minerals for wet chemical analyses was not feasible because of many small mineral inclusions, such as leucoxene and ore minerals. Even a reasonably clean fraction of blue-green amphibole that has been chemically analyzed (Hietanen, 1973, Table 1a, anal. 796h) contained a few colorless amphibole grains. The major constituents—amphiboles, epidote minerals, plagioclase, and chlorite—were therefore analyzed by electron microprobe by G. K. Czamanske. In each sample, several grains of optically different types of amphibole and epidote minerals were chosen for analyses (Tables 2a and 3). Chlorite was analyzed in five samples (Table 4), and plagioclase in six (Table 5).

Some of the accessory minerals, such as ilmenite in sample 551, sphene in samples 532 and 465, and leucoxene in samples 463 and 532, were checked

with the electron microprobe for their Ti, Mn, and Mg contents. Leucoxene was found to consist of 93 to 98 percent TiO_2.

Analytical Techniques
by G. K. Czamanske

Grains of albite, amphibole, chlorite, epidote, and zoisite in carbon-coated, polished thin sections were analyzed with an ARL EMX-SM electron microprobe. Accelerating potentials were chosen to minimize effects of interferences on the important light constituents Al, Mg, and Si (see Desborough and Heidel, 1971). The following analytical conditions were used: Ca, Fe, Na were run at 15 kilovolts, whereas Si, K, Al and Mn, Ti, Mg were run at 10 kilowatts. Sample current on benitoite was 0.2 μ amperes at 15 kilowatts and 0.03 μ amperes at 10 kilovolts, with a beam diameter of 2 to 3 microns. Typically, 6 to 12 points per grain were analyzed for each set of three elements, for counting intervals of about 10 seconds (actual count intervals were fixed by beam current termination). Raw count data were corrected for drift, background, absorption, fluorescence, and atomic number with the aid of the Fortran IV computer program of Beeson (1967).

Standards for albite, epidote, and zoisite were the following oxides: Al_2O_3, Fe_2O_3, MgO, MnO_2, SiO_2, TiO_2, and the following three silicates from Goldich, Ingamells, Suhr, and Anderson (1967): albite from Amelia County, Virginia (Na), Or-1 (K), and Px-1. For the amphiboles, a homogeneous, hastingsitic amphibole [$Na_{0.62}$ $K_{0.29}$ $Ca_{1.79}$ ($Al_{0.18}$ $Fe^{3+}_{0.62}$ $Ti_{0.37}$ $Mg_{1.02}Fe^{2+}_{2.88}Mn_{0.06})_{5.13}Si_{6.26}Al_{1.72}O_{22}OH)_2$] was employed. A homogeneous biotite [$K_{1.89}Na_{0.07}Ba_{0.03}$ ($Mg_{4.39}$ $Fe^{2+}_{1.08}$ $Mn_{0.02}$ $Al_{0.01}$ $Fe^{3+}_{0.28}$ $Cr_{0.03}$ $Ti_{0.18})_{5.99}$ $Si_{5.72}Al_{2.26}O_{20}(OH)_4$] was used to analyze the chlorites, with the amphibole above as a Ca standard. Both the amphibole and biotite were analyzed by wet chemical techniques by C. O. Igamells, have been checked on the microprobe against many other superior standards, and are routinely used as standards because of their purity and homogeneity.

For purposes of comparison and further calculation, oxide weight percentage values reported in Tables 2, 3, 4, and 5 are consistently reported to two decimal places, although in terms of expected accuracy, no more than three significant figures can be justified, *e.g.*, SiO_2 will be reported as 42.97 rather than 43.0. In all tables 0.0 means less than 0.005.

Some of the spot analyses that consisted of highly inhomogeneous counts were split into two parts: the

TABLE 2a.   Electron Microprobe Analyses, in Weight Percent, of Amphiboles from Metamorphic Rocks, Feather River Area
Analyst, G. K. Czamanske, U. S. Geological Survey

Sample Rock	796 Metagabbro									546 Metagabbro		551 Metabasalt		
Analyzed part	Blue green rim	Small prism	High Al counts for 4	Colorless core					Low Al counts for 4	Prism		Prism	Core of 15	High Al counts for 16
										core	end			
Anal.	1	2	3	4	5	6	7	8	9	10	11	12	13	14
SiO_2	42.97	43.94	42.82	51.31	53.31	57.16	56.43	56.65	55.75	52.10	55.29	42.49	42.58	41.35
Al_2O_3	16.11	14.93	14.93	6.17	4.55	4.03	3.61	2.78	1.09	5.14	2.09	13.92	11.65	13.77
TiO_2	0.19	0.15	0.25	0.13	0.09	0.06	0.10	0.08	0.04	0.34	0.20	0.36	0.29	0.42
Fe_2O_3	2.63	2.45	1.88	1.55	1.80	1.44	1.71	1.48	1.33	2.66	2.24	4.35	4.75	4.53
FeO	9.47	8.82	6.77	5.59	6.49	5.20	6.16	5.34	4.80	9.58	8.05	15.69	17.10	16.33
MgO	12.76	13.70	13.96	18.10	18.90	20.47	20.34	20.58	20.64	15.37	18.13	7.65	8.00	7.02
MnO	0.23	0.21	0.06	0.12	0.27	0.18	0.19	0.20	0.13	0.30	0.29	0.35	0.31	0.34
CaO	11.72	11.91	12.22	12.55	11.76	12.33	12.33	12.23	12.77	11.59	11.66	11.50	11.18	11.45
Na_2O	1.92	1.87	0.94	0.54	0.58	0.80	0.38	0.37	0.28	0.63	0.18	1.29	1.10	1.28
K_2O	0.28	0.19	0.21	0.03	0.02	0.00	0.00	0.00	0.00	0.02	0.00	0.34	0.37	0.28
Total	98.28	98.17	94.04	96.09	97.77	101.67	101.25	99.71	98.83	97.73	98.13	97.94	97.33	96.77
Mg/Fe	1.922	2.214	2.936	4.619	4.157	5.617	4.711	5.501	6.132	2.290	3.210	0.695	0.667	0.613
Fe/Al	0.521	0.524	0.403	0.803	1.265	1.144	1.513	1.703	3.902	1.652	3.417	1.000	1.302	1.051

Sample Rock	551 Metabasalt		463 Meta-andesite		465 Metadiorite				532 Metadiorite			464 Metadacite			
Analyzed part	Rim of 13	Low Al counts for 14	Green hornblende		Green hornblende				Green hornblende			High Al counts for 28	Small prism	Low Al counts for 26	Simple grain
Anal.	15	16	17	18	19	20	21	22	23	24	25	26	27	28	29
SiO_2	50.76	51.64	47.30	48.14	47.64	48.31	48.82	49.79	48.31	47.89	49.08	47.54	50.99	56.58	56.50
Al_2O_3	2.64	2.40	8.02	6.84	7.55	7.20	6.39	5.76	7.43	7.40	6.48	6.76	4.85	0.81	0.88
TiO_2	0.11	0.07	1.48	1.34	1.14	1.11	1.33	1.29	0.86	0.83	0.88	0.24	0.25	0.15	0.03
Fe_2O_3*	4.01	3.78	2.70	2.56	2.98	3.10	3.16	3.00	2.91	2.90	2.89	2.01	2.26	1.47	1.40
FeO	14.44	13.61	9.71	9.23	10.74	11.20	11.40	10.80	10.48	10.47	10.40	7.23	8.12	5.29	5.04
MgO	12.00	12.13	15.59	16.22	14.92	14.54	14.83	14.84	14.35	14.50	14.71	18.21	16.71	19.32	20.47
MnO	0.21	0.19	0.25	0.23	0.31	0.40	0.43	0.42	0.44	0.37	0.44	0.16	0.20	0.19	0.18
CaO	12.06	11.77	10.25	11.19	10.69	10.49	10.35	10.48	11.02	11.21	11.08	12.51	12.54	13.11	13.28
Na_2O	0.36	0.67	1.03	1.10	1.30	1.10	1.02	1.13	1.23	1.21	1.21	0.48	0.19	0.12	0.06
K_2O	0.11	0.12	0.08	0.09	0.10	0.03	0.05	0.09	0.14	0.18	0.07	0.01	0.06	0.00	0.00
Total	96.70	96.38	96.41	96.94	97.37	97.48	97.78	97.60	97.17	96.96	97.24	95.15	96.17	97.04	97.83
Mg/Fe	1.185	1.272	2.290	2.506	1.981	1.853	1.855	1.959	1.953	1.976	2.016	3.591	2.933	5.209	5.797
Fe/Al	4.849	5.021	1.079	1.197	1.261	1.379	1.583	1.663	1.251	1.253	1.424	0.949	1.486	5.786	5.064

*20% of total Fe expressed as Fe_2O_3

TABLE 2b. Structural Formulas for Amphiboles in Table 2a on Anhydrous Basis of 23(O)

Site Total ions		Tetrahedral Σ = 8.00		M(1)--M(3) Σ = 5.00						M(4) Σ = 2.00				A		
Sample	Anal	Si	Al	Al	Fe^{3+}	Ti	Mg	Fe^{2+}	Mn	Fe^{2+}	Mn	Ca	Na	Na	K	Ca
796	1	6.200	1.800	0.939	0.286	0.021	2.744	1.010		0.133	0.028	1.812	0.027	0.510	0.052	
	2	6.319	1.681	0.849	0.265	0.016	2.937	0.933		0.128	0.026	1.835	0.011	0.510	0.035	
	3	6.346	1.654	0.954	0.210	0.028	3.083	0.725		0.114	0.008	1.878		0.271	0.039	0.063
	796*	6.334	1.666	0.810	0.404	0.023	2.822	0.934	0.007		0.012	1.902	0.086	0.449	0.043	
	4	7.320	0.680	0.358	0.166	0.014	3.849	0.613		0.054	0.015	1.918	0.013	0.136	0.006	
	5	7.484	0.516	0.237	0.190	0.009	3.955	0.609		0.153	0.032	1.769	0.046	0.112	0.004	
	6	7.636	0.364	0.271	0.145	0.006	4.076	0.502		0.079	0.020	1.765	0.136	0.072		
	7	7.611	0.389	0.185	0.173	0.010	4.089	0.543		0.152	0.022	1.782	0.044	0.055		
	8	7.720	0.280	0.167	0.152	0.008	4.180	0.493		0.115	0.023	1.786	0.076	0.022		
	9	7.827	0.173	0.007	0.141	0.004	4.319	0.529		0.034	0.016	1.921	0.029	0.047		
546	10	7.443	0.557	0.308	0.285	0.036	3.273	1.098		0.047	0.036	1.774	0.143	0.031	0.004	
	11	7.765	0.235	0.111	0.237	0.021	3.795	0.836		0.109	0.035	1.755	0.049			
551	12	6.360	1.640	0.816	0.490	0.041	1.707	1.946		0.018	0.044	1.844	0.094	0.281	0.065	
	**	6.385	1.615	0.850	0.312	0.041	1.714	2.083		0.069	0.044	1.852	0.035	0.341	0.065	
	13	6.472	1.528	0.559	0.543	0.033	1.813	2.052		0.121	0.040	1.821	0.018	0.306	0.072	
	**	6.509	1.491	0.608	0.347	0.033	1.823	2.189		0.196	0.040	1.831		0.326	0.072	0.067
	14	6.303	1.697	0.777	0.520	0.048	1.595	2.060		0.021	0.044	1.870	0.065	0.314	0.054	
	**	6.316	1.684	0.794	0.330	0.049	1.598	2.276		0.047	0.044	1.874	0.035	0.344	0.054	
	15	7.563	0.437	0.027	0.450	0.012	2.665	1.799	0.027			1.925	0.075	0.029	0.021	
	**	7.591	0.409	0.056	0.286	0.013	2.675	1.970			0.027	1.933	0.040	0.064	0.021	
	16	7.670	0.330	0.090	0.423	0.008	2.685	1.690	0.024			1.873	0.127	0.066	0.023	
	**	7.698	0.302	0.120	0.269	0.008	2.695	1.852	0.024			1.880	0.120	0.074	0.022	
463	17	6.901	1.099	0.280	0.296	0.162	3.390	0.872		0.313	0.031	1.602	0.054	0.238	0.015	
	18	6.986	1.014	0.156	0.280	0.146	3.509	0.909		0.211	0.028	1.740	0.021	0.289	0.017	
465	19	6.936	1.064	0.232	0.326	0.125	3.238	1.079		0.229	0.038	1.668	0.065	0.302	0.019	
	20	7.023	0.977	0.256	0.339	0.121	3.151	1.133		0.229	0.049	1.634	0.088	0.222	0.006	
	21	7.079	0.921	0.171	0.345	0.145	3.205	1.134		0.249	0.053	1.608	0.090	0.197	0.009	
	22	7.203	0.797	0.185	0.327	0.140	3.200	1.148		0.159	0.052	1.624	0.165	0.152	0.017	
532	23	7.035	0.965	0.310	0.319	0.094	3.115	1.162		0.114	0.054	1.719	0.113	0.235	0.026	
	24	7.000	1.000	0.274	0.319	0.091	3.159	1.157		0.123	0.046	1.755	0.076	0.267	0.034	
	25	7.132	0.868	0.241	0.316	0.096	3.186	1.161		0.103	0.054	1.725	0.118	0.223	0.013	
464	26	6.971	1.029	0.139	0.222	0.027	3.980	0.633		0.254	0.020	1.726		0.137	0.002	0.239
	27	7.376	0.624	0.202	0.246	0.027	3.603	0.922		0.061	0.024	1.915		0.053	0.011	0.029
	28	7.934	0.066	0.068	0.155	0.016	4.038	0.620	0.023			1.970	0.030	0.002		
	29	7.859	0.141	0.004	0.147	0.003	4.244	0.586	0.016		0.005	1.979	0.016			
2043		6.43	1.57	0.~1	0.51	0.06	1.93	1.89		0.08	0.03	1.70	0.19	0.47	0.06	0.53

*Wet chemical analyses from Hietanen (1973)

**The number of ions given on lower line are recalculated for Fe_2O_3 = 12.7% of total FeO

high Al and high Fe counts were combined with the low Mg counts to form one analysis and the low Al, low Fe, and high Mg counts were calculated as separate analysis. Analyses 3 and 9 were derived from analysis 4 in this way. Analyses 14 and 16 are based on splitting counts from two grains and combining high Al and Fe counts with low Mg counts for 14 and low Al and Fe counts with high Mg counts for 16. Analysis 28 represents low Al and low Fe counts combined with high Mg counts, and analysis 26 high Al and high Fe counts combined with low Mg counts from the same grain.

Amphiboles

The composition of analyzed amphiboles (Table 2a) ranges from actinolite through actinolitic hornblende to a hornblende rich in aluminum, some rocks containing the two end members and some others intermediate compositions. Some of the intermediate compositions are averages of inhomo-

TABLE 3. Composition of Epidote Minerals in Metamorphic Rocks, Feather River Area[1]

Sample	796					546	551			463		465		532			466					
Rock	Metagabbro					Meta-gabbro	Metabasalt			Meta-andesite		Metadiorite		Metadiorite			Metadacite					
Mineral	Zoisite		Clinozoisite			Epidote	Epidote			Epidote		Epidote		Epidote			Clinozoisite		Epidote			
Anal.	30	31	32	33	34	35	36	37	38	39	40	41	42	43	44	45	46	47	48	49	50	51
SiO_2	41.52	41.64	40.03	39.98	39.69	38.75	39.07	39.23	39.10	39.70	38.28	39.28	39.26	38.40	39.81	39.08	39.44	39.47	39.86	38.11	38.10	37.57
Al_2O_3	33.07	33.38	32.05	30.91	30.21	24.86	27.08	27.77	27.17	28.99	24.23	26.31	26.35	27.42	27.26	26.96	29.61	29.32	28.43	25.23	22.65	23.12
Fe_2O_3*	0.23	0.11	2.34	3.58	4.87	11.58	8.27	8.72	11.65	5.76	12.68	9.27	9.95	8.09	8.38	8.63	4.64	5.29	6.24	10.87	12.85	13.14
TiO_2	0.01	0.02	0.03	0.01	0.04	0.06	0.08	0.08	0.08	0.07	0.31	0.10	0.14	0.05	0.09	0.03	0.11	0.04	0.08	0.05	0.25	0.03
MgO	0.01	0.00	0.00	0.00	0.04	0.00	0.00	0.00	0.00	0.04	0.04	0.01	0.01	0.00	0.00	0.00	0.02	0.0	0.0	0.0	0.00	0.0
MnO	0.05	0.05	0.08	0.07	0.11	0.23	0.04	0.00	0.04	0.19	0.27	0.10	0.16	0.17	0.24	0.06	0.0	0.10	0.0	0.07	0.17	0.10
CaO	23.42	23.97	23.89	24.12	24.24	23.07	23.39	23.24	20.66	23.71	22.53	23.39	23.47	23.31	23.34	23.08	24.11	24.22	23.85	23.06	22.76	22.82
Na_2O	0.46	0.45	0.00	0.00	0.00	0.00	0.00	0.00	0.00	0.00	0.00	0.00	0.00	0.00	0.00	0.00	0.0	0.0	0.0	0.0	0.0	0.0
K_2O	0.02	0.05	0.04	0.01	0.00	0.02	0.07	0.07	0.07	0.06	0.06	0.07	0.09	0.04	0.06	0.07	0.03	0.07	0.09	0.02	0.04	0.09
Total	98.79	100.62	98.46	98.68	98.20	98.57	98.00	99.11	98.77	98.52	98.40	98.53	99.43	97.48	99.18	97.91	97.96	98.51	98.55	97.41	96.52	96.87

Number of ions on anhydrous basis (25 oxygen atoms per 2 formula units)

Si	3.100	3.084	3.031	3.037	3.017	3.036	3.041	3.018	3.023	3.046	3.017	3.051	3.031	3.007	3.059	3.045	3.034	3.029	3.061	3.016	3.059	3.020
Al	2.911	2.917	2.860	2.767	2.706	2.296	2.484	2.518	2.475	2.622	2.251	2.409	2.398	2.531	2.469	2.476	2.685	2.652	2.573	2.353	2.143	2.191
Fe^{+3}	0.013	0.006	0.133	0.204	0.279	0.683	0.485	0.505	0.678	0.333	0.752	0.542	0.578	0.477	0.485	0.506	0.269	0.305	0.360	0.647	0.777	0.795
Ti	0.0	0.001	0.002	0.0	0.002	0.004	0.005	0.005	0.005	0.004	0.019	0.006	0.008	0.003	0.005	0.001	0.006	0.002	0.005	0.003	0.015	0.002
Mg	0.001	0.0	0.0	0.0	0.004	0.0	0.0	0.0	0.0	0.005	0.004	0.002	0.001	0.0	0.0	0.0	0.0	0.0	0.0	0.0	0.0	0.0
Mn	0.003	0.003	0.005	0.004	0.007	0.015	0.003	0.0	0.003	0.012	0.018	0.006	0.011	0.011	0.015	0.004	0.001	0.007	0.0	0.005	0.017	0.007
Ca	1.874	1.904	1.938	1.963	1.974	1.937	1.951	1.916	1.711	1.949	1.902	1.947	1.941	1.955	1.922	1.927	1.987	1.991	1.963	1.955	1.958	1.966
Na	0.067	0.064	0.0	0.00	0.0	0.0	0.0	0.0	0.0	0.0	0.0	0.0	0.0	0.0	0.0	0.0	0.0	0.0	0.0	0.0	0.0	0.0
K	0.001	0.004	0.004	0.001	0.0	0.002	0.007	0.007	0.007	0.006	0.006	0.007	0.008	0.004	0.006	0.007	0.003	0.007	0.009	0.002	0.004	0.009

Pistacite content in molecular percent

$\dfrac{Fe^{3+}}{Fe^{3+}+Al}$ 0.44   0.21   4.44   6.87   9.35   22.93   16.34   16.71   21.50   11.27   25.04   18.37   19.42   15.86   16.42   16.97   9.11   10.31   12.27   21.57   26.61   26.62

Fe/Al   0.004   0.002   0.047   0.074   0.103   0.297   0.195   0.200   0.274   0.127   0.334   0.225   0.241   0.189   0.196   0.204   0.100   0.115   0.140   0.275   0.362   0.362

*Total Fe as Fe_2O_3

[1] *Electron microprobe analyses, in weight percent, by G. K. Czamanske, U. S. Geological Survey.*

geneous counts; they include analysis spots with high Al and low Al counts, as well as spots with high Fe and low Fe counts. Comparison of the split analyses from inhomogeneous grains with the analyses from homogeneous grains in the same sample shows that the high Al and Fe counts combined with low Mg counts give composition of blue green or green hornblende (anal. 3, 14, and 26) whereas the low Al and Fe counts combined with high Mg counts (anal. 9, 16, and 28) give composition of actinolite. This similarity of analyses based on selected counts with the analyses of homogeneous grains in the same sample supports the possibility of bimodal composition of grains that give inhomogeneous counts. It seems likely that submicroscopic intergrowths of actinolite and hornblende, similar to those seen under the microscope although not detectable optically, may give rise to the inhomogeneity of counts.

In all probe analyses, 20 percent of total Fe was calculated as Fe_2O_3 to agree with the approximate $Fe_2O_3(FeO + Fe_2O_3)$ ratio in the host rocks after an allowance to form epidote and accessories was made. In the wet chemical analysis of blue-green hornblende in sample 796, this ratio is 0.32 (Hietanen, 1973, Table 1a, anal. 796h). This analysis was recalculated on anhydrous basis of 23(O) and is shown in Table 2a under *796. The two probe analyses (1 and 2) of high Al grains in the same sample are similar to this wet chemical analysis, all three having about 1.9 percent Na_2O and 15 to 16 percent Al_2O_3. Analyses 12 to 16 for the amphiboles in sample 551 were also calculated for $Fe_2O_3 = 12.7$ percent of total FeO to conform with the lower $Fe^{3+}/(Fe^{2+} + Fe^{3+})$ ratio in the rock analysis (anal. 551, Hietanen, 1973, see also Fig. 6).

Structural Formulae

Differences in the composition of analyzed amphiboles can be best compared on the basis of structural formulas based on crystal chemistry and X-ray work (Table 2b). According to the method of calculation by Papike *et al.* (1969), all Si and a part of Al are assigned to the eight tetrahedral sites. The remaining Al, Ti and Fe^{3+} together with Mg, Fe^{2+} and Mn occupy the five octahedral sites $M(1)$, $M(2)$, and

TABLE 4. Composition of Chlorite and Muscovite in Metamorphic Rocks, Feather River Area*

	Chlorite								Musco-vite
Sample	796	546	463		465		464		796
Rock	Metagabbro		Meta-andesite		Metadiorite		Metadacite		Meta-gabbro
Anal.	52	53	54	55	56	57	58	59	60
SiO₂	27.69	25.99	26.28	26.52	27.46	26.98	26.00	23.31	47.18
Al₂O₃	22.99	21.77	21.07	20.70	21.23	21.18	21.03	20.85	34.76
Fe₂O₃	1.11	1.11	1.11	1.11	1.11	1.11	1.11	1.11	0.0
TiO₂	0.0	0.06	0.04	0.02	0.05	0.04	0.07	0.0	0.04
MgO	25.40	19.51	18.68	18.74	21.19	21.45	21.51	22.71	1.13
FeO	9.23	17.38	18.26	18.58	15.16	15.19	13.17	12.29	0.61
MnO	0.15	0.21	0.31	0.30	0.29	0.27	0.23	0.22	0.0
Na₂O	0.0	0.0	0.01	0.00	0.0	0.0	0.01	0.01	0.39
K₂O	0.0	0.0	0.0	0.02	0.0	0.0	0.0	0.01	10.25
Total	86.57	86.03	85.76	85.99	86.49	86.22	83.13	83.51	94.35

Number of ions on anhydrous basis of 28(O) for chlorite and 22(O) for muscovite

Si	5.423	5.367	5.472	5.515	5.561	5.489	5.440	5.455	6.291
Al	2.577	2.633	2.529	2.485	2.460	2.512	2.560	2.545	1.709
Al	2.729	2.664	2.641	2.588	2.627	2.568	2.627	2.549	3.755
Fe^{+3}	0.164	0.173	0.174	0.174	0.169	0.170	0.175	0.173	0.0
Ti	0.0	0.009	0.006	0.003	0.007	0.006	0.011	0.0	0.004
Mg	7.413	6.006	5.796	5.808	6.395	6.506	6.709	7.018	0.224
Fe	1.511	3.001	3.179	3.231	2.568	2.585	2.304	2.131	0.068
Mn	0.025	0.037	0.054	0.052	0.049	0.046	0.041	0.038	0.0
Na	0.0	0.0	0.002	0.001	0.0	0.0	0.003	0.004	0.100
K	0.0	0.0	0.0	0.004	0.0	0.0	0.0	0.003	1.743
Mg/Mg+Fe^{+2}	0.831	0.667	0.646	0.643	0.714	0.716	0.744	0.767	0.767
Mg/Fe total	4.424	1.892	1.729	1.706	2.337	2.361	2.705	3.044	3.176

Electron microprobe analyses, in weight percent, by G. K. Czamanske, U.S. Geological Survey.

$M(3)$. A small deficiency in these sites in analyses 16 and 28 is considered to be due partly to an analytical error (both are composite of low Al counts) and partly to the presence of Cr and V or some other element not analyzed. The remaining Mn and some Fe occupy, together with Ca and possibly Na, the two $M(4)$ sites. The A-site is either vacant (as in actinolite) or is occupied by Na and K (including some Ca in three analyses), and the total occupancy together with the excess of the octahedral valences (Al^{3+} + Fe^{3+} + Ti^{4+}), balances the negative charge of the tetrahedral sites (Al^{iv}). According to this scheme, the results of calculation on an anhydrous basis of 23(O) from the U.S. Geological Survey computer program E210 are shown in Table 2b. A generalized formula for the blue-green high-Al amphibole is $(Na,K)_{0.5}Ca_2Mg_{2.8}Fe^{2+}_{1.0}Al_{0.9}Fe^{3+}_{0.8}Al_{1.7}Si_{6.3}O_{22}(OH)_2$. The green amphibole has the generalized formula: $(Na,K)_{0.5}Ca_2Mg_{3.2}Fe^{2+}_{1.2}Al_{0.2}Ti_{0.1}Fe^{3+}_{0.3}AlSi_7O_{22}(OH)_2$. In both formulas Mn, Fe^{2+}, and Na, substitute for some of the Ca, so that the total of Ca + alkalies ranges from 1.9 to 2.5. Most actinolites have Mg/(Fe + Mg) ratios of 0.75 to 0.85; in the metabasalt (sample 551), however,

this ratio is 0.55, reflecting the high content of iron in the host rock.

Both generalized formulas are derived from tremolite mainly by two coupled substitutions that, in completion, would lead to the compositions of edenite and tschermakite. The extent of these coupled substitutions differs; in the formula unit of green hornblende, the edenitic substitution ($Na^A Al^{iv} \rightleftharpoons \square^A Si^{iv}$) is 0.3, and the tschermakitic substitution ($Al^{vi}Al^{iv} \rightleftharpoons Mg^{vi},Si^{iv}$) is 0.7. In the blue-green hornblende in sample 796, the corresponding values are 0.5 and 1.2, and in sample 551 they average 0.4 and 1.1. However, the ratio of the edenitic substitution to the tschermakitic substitution remains constant and close to 3:7. For this scheme of two coupled substitutions, the end member would be hornblende $Na_{0.6}Ca_2(Mg,Fe^{2+})_{3.6}(Al,Fe^{3+})_{1.4}Al_2Si_6O_{22}(OH)_2$ in which edenitic substitution is 0.6 and tschermakitic substitution is 1.4. Such a composition is identical to the end member composition suggested by Robinson, Ross, and Jaffe (1971) on the basis of a more generalized study. Since the same amount (20 percent) of total Fe^{2+} was changed to Fe^{3+} in all

TABLE 5. Composition of Plagioclase in Metamorphic Rocks, Feather River Area*

Sample	796	546	551		463	532	464	
Rock	Metagabbro		Metabasalt		Meta-andesite	Meta-diorite	Metadacite	
Anal.	61	62	63	64	65	66	67	68
SiO₂	46.37	50.66	69.02	69.49	69.31	69.22	68.72	69.85
Al₂O₃	35.54	31.45	20.38	20.02	20.03	19.95	19.91	19.60
TiO₂	0.0	0.0	0.0	0.03	0.04	0.14	0.0	0.0
FeO	0.0	0.0	0.16	0.09	0.0	0.01	0.0	0.0
MnO	0.0	0.0	0.0	0.0	0.0	0.21	0.0	0.0
CaO	18.50	14.42	0.66	0.57	0.47	0.48	0.42	0.38
Na₂O	0.67	3.23	11.59	11.58	11.57	11.59	11.58	11.64
K₂O	0.03	0.03	0.10	0.02	0.02	0.03	0.02	0.02
Total	100.11	99.79	101.91	101.80	100.44	101.63	100.65	101.49

Number of ions on basis of 32(O)

Si	8.514	9.236	11.861	11.933	11.936	11.917	11.931	12.14
Al	7.475	6.758	4.129	4.052	4.064	4.049	4.069	3.973
Ti	0.0	0.0	0.0	0.004	0.005	0.018	0.0	0.0
Fe	0.0	0.0	0.023	0.014	0.0	0.001	0.0	0.0
Mn	0.0	0.0	0.0	0.0	0.0	0.031	0.0	0.0
Ca	3.639	2.817	0.121	0.105	0.086	0.088	0.077	0.070
Na	0.237	1.141	3.861	3.856	3.865	3.868	3.897	3.881
K	0.006	0.007	0.021	0.004	0.005	0.007	0.004	0.004

Molecular percentage

An	93.742	71.061	3.022	2.658	2.169	2.216	1.941	1.775
Ab	6.108	28.769	96.452	97.231	97.714	97.602	97.959	98.131
Or	0.151	0.170	0.526	0.111	0.117	0.183	0.100	0.094

Electron microprobe analyses, in weight percent, by G. K. Czamanske, U. S. Geological Survey.

probe analyses, the positions of points in the graphs are only approximate.

Calculation of the analyses from sample 551 (Table 2b) shows that lowering of the Fe_2O_3 content from 20 to 12.7 percent lowers the Al^{iv} value by 0.03 and increases the A-site occupancy by the same amount, but that the total alkalies remain constant. Therefore much of the discrepancy in alkali/Al^{iv} ratio due to errors in estimation of Fe^{3+} can be avoided if total alkalies instead of A-site occupancy are plotted against the tetrahedral Al content (Fig. 4). In Figure 4 all points fall close to a trend line that connects the average for the blue-green hornblende to the origin. The ratio of total alkalies to the tetrahedral Al content thus remains constant and close to 1:3. This trend leads to an extreme member marked by point "Hornblende" on the line connecting pargasite to tschermakite. Alkali content of the "Hornblende" is 0.66 and it has 2 tetrahedral Al. The analysis 26, which falls far below the trend line, has 0.24 Ca ions in the A-site, whereas in most analyses Ca content is lower than 2 and some Na enters the $M(4)$ sites. The A-site occupancy is thus generally somewhat lower than the total alkali content. In "Hornblende" the A-site occupancy is
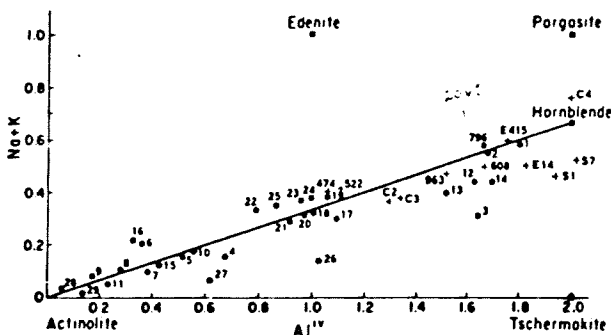
FIG. 4. Plot of total alkalies against tetrahedral Al per formula unit on basis of 23(O) for actinolite and hornblende. Numbers 1 to 29 refer to microprobe analyses of Table 2. The others, added for comparison, are by wet chemical methods and were recalculated on the anhydrous basis of 23(O) per formula unit. Point 796 is for the wet chemical analysis of blue-green hornblende in sample 796 (Hietanen, 1973). Analysis points 522 and 474 are for hornblendes in the plutonic rocks in the study area (Hietanen, 1971); C2, C3, and C4 are for three amphiboles from the neighboring Bidwell Bar area (Compton, 1958); E14 and E415 are for hornblende from the Emeryville area, Adirondack Mountains, New York (Engel and Engel, 1962); 963 is for hornblende in garnet amphibolite and 608 for hornblende in kyanite-bearing rock, Idaho (Hietanen, 1963); S1 and S7 are for hornblende from Airola, Switzerland (Steiger, 1961).

0.6 and the ratio $(Na + K)^A/Al^{iv} = 0.3$, which value is only a little lower than the ratio of the total alkalies to the tetrahedral Al.

The ratio of octahedral Al + Fe^{3+} + Ti to tetrahedral Al (Fig. 5) is close to 0.7 for most analyzed hornblende grains. A nearly similar ratio was suggested by Leake (1965a, b) for the maximum possible Al^{ri} content in Ca-amphiboles in general. Only analysis point 26 in the Feather River area falls significantly below the trend line. This analysis combines high Al, high Fe, and low Mg counts from a spot, and therefore the possibility of analytical error is larger than in the analysis from homogeneous areas. Analysis 26 shows an exceptionally large amount of Ca and a low amount of alkalies. For comparison, two wet chemical analyses of hornblende in the plutonic rocks (Hietanen, 1971, Table 1, anal. 474 and 522) were plotted on Figures 4 and 5. The ratio of alkalies to tetrahedral Al is similar to that in the green hornblende in the metamorphic rocks; the octahedral Al + Fe^{3+} + Ti content and the extent of tschermakitic substitution, however, are higher.

Comparison with the Published Analyses

Compton (1958) studied amphiboles from the contact aureole of the Bald Rock pluton located 10 to 20 miles south-southwest of Granite Basin pluton. Three of his analyses were recalculated on an anhydrous basis of 23(O) and plotted in Figures 4 and 5 (Anal. points C-2, C-3, and C-4). Two of these analyses (C-2, C-3) have Al^{iv} contents intermediate between the green and blue-green hornblende near Granite Basin pluton (Fig. 4); the third (C-4) has a composition closer to hastingsite than any other amphibole in this region. The host rocks for these three analyses are basaltic intrusive and extrusive rocks similar to those of this study. Klein (1969) made electron microprobe analyses of amphiboles in four other specimens collected by Compton from the southwestern contact aureole of the Bald Rock pluton. The mineralogy given by him is similar to that in the low grade zone near Granite Basin except that only epidote, but no clinozoisite, was reported. On the basis of textural relations, Klein suggested that actinolite and hornblende may have crystallized in equilibrium. Klein's analyses 2-6 and 2-7 for the hornblende in metadolerite are similar to the green hornblende in sample 551 in Granite Basin and analysis 2-5 is close to the composition of hornblende in sample 465.

Leake (1965a, b, 1968, 1971) has compiled nearly 1500 analyses of calciferous and subcalciferous amphiboles from the literature and has concluded that the content of Al^{vi} is controlled by rock composition and pressure and that the maximum possible Al^{vi} increases as Al^{iv} increases. He has also suggested a nomenclature based on Si and Ca + Na + K contents in the half-unit cell. The analyses of the blue-green hornblende in the Feather River area fall within tschermakitic hornblende, and those of the green hornblende within magnesio-hornblende in his scheme. These names are not adopted here because of chemical features (Figs. 4 and 5) that bring the blue-green hornblende closer to the pargasite type than to the tschermakite type hornblende. Ernst (1968) uses the name pargasite for $NaCa_2Mg_4$ $AlSi_6Al_2O_{22}(OH)_2$ and the name hastingsite for the corresponding ferrous ferric end member $NaCa_2Fe^{2+}_4$ $Fe^{3+}Si_6Al_2O_{22}(OH)_2$. In the blue-green hornblende analyzed chemically (anal. 796), the extent of substitution of Mg by Fe^{2+} and that of octahedral Al by Fe^{3+} are both 1:4. Thus the end member called pargasite in the graphs (Figs. 4 and 5) actually is a member that consists of 3/4 pargasite and 1/4 hastingsite, using the nomenclature of Ernst (1968) and Phillips and Layton (1964).

Robinson, Ross, and Jaffe (1971, Fig. 8) have plotted A-site occupancy against tetrahedral Al for a large number of hornblende analyses selected from the literature. The trend in their diagram is remarkably similar to the trend in Figure 4 of this paper, except for a much greater scatter of points. This scatter is probably due mainly to differences in environments of crystallization because these analyses represent a collection of Ca-amphiboles from various geologic environments and diverse PT conditions. For comparison, two analyses of green hornblende from an anorthosite area in Idaho (Hietanen, 1963, anal. 608, p. 43, and anal. of hornblende in sample 963, p. 33) are plotted in Figures 4 and 5. These hornblendes crystallized at the pressure of the triple point of kyanite, andalusite, and sillimanite (~5 kbar) and plot under (in Fig. 4) or above (in Fig. 5) the trend line for the hornblendes in the Feather River area, where the pressure of crystallization was lower (~4 kbar). The ratio of A-site occupancy to tetrahedral Al for these hornblendes is 1:4. Similar ratios (1:4 and 1:5) were calculated for two analyzed gedrites in this area (Hietanen, 1959, 1963).

Added for comparison in Figure 4 are two analyses (E-14 and E-415) for blue-green hornblende

from Emeryville, Adirondack Mountains, New York (Engel and Engel, 1962) and two (S-1, S-7) for hornblende in the Tremola series, Switzerland (Steiger, 1961). Metamorphism in Emeryville was in the amphibolite facies and in medium pressures, whereas the Tremola series recrystallized at higher pressures as shown by the occurrence of staurolite and kyanite in the pelitic layers south of St. Gotthard (Hezner, 1909; Hafner, 1958). The ratio of (Na + K)^A/Al^{iv} for the hornblende analysis S-1 is 1:7, indicating a much higher content of tschermakite molecule than is present in the other hornblende analyses shown in Figure 4. Frey (1969, p. 68) gives two analyses of hornblende in kyanite-bearing rock at Frodalera, south side of St. Gotthard massive. These and a partial reanalysis of one of them given by Leake (1971, p. 394) confirm the high content of tschermakite in the hornblendes of this area.

Iron, Magnesium, and Titanium Contents

The iron-magnesium ratio and the titanium content of amphiboles depend more closely on the Fe, Mg, and Ti contents of the host rocks than on the grade of metamorphism.

The Mg/(Fe + Mg) ratio shows considerable variation but generally decreases slightly with increasing tetrahedral Al. All the actinolites are rich in magnesium. The amphibole pairs—the Al-rich hornblende and actinolite—in the metabasalt (Sp.
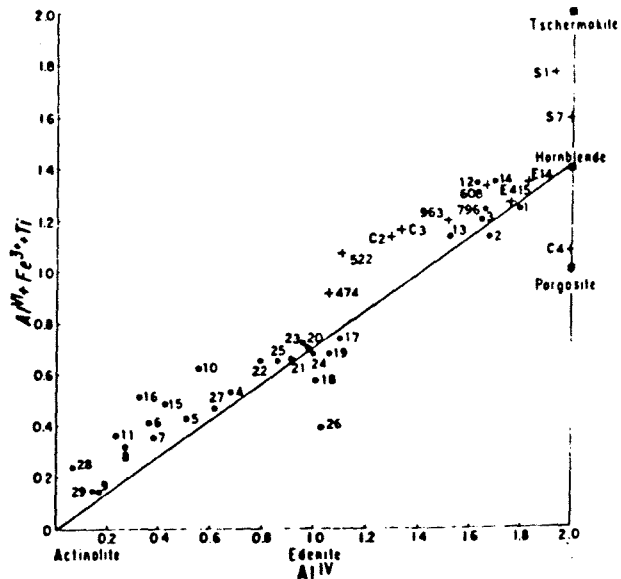

FIG. 5. Plot of octahedral Al + Fe^{3+} + Ti against tetrahedral Al per 23(O). Numbers refer to the same analyses as those in Figure 4.

551) are richer in iron than any other amphibole. This is due to the bulk composition of the meta-basalt, which has Fe/Mg = 1, whereas in all the other host rocks this ratio is less than 1/2 (Hietanen, 1973). Compton's (1958) hastingsite (C-4) with only one Mg substituting for Fe^{2+} is from an iron-rich layer in metabasalt east of Feather Falls.

To test the possible influence of oxygen fugacity on the Mg/(Mg + Fe) ratio of hornblende, this ratio was plotted against $Fe^{3+}/(Fe^{2+} + Fe^{3+})$ in the host rocks (Fig. 6). Separate curves were drawn by visual inspection for amphiboles with high, low, and median Al contents. In each of the amphibole groups the Mg/(Mg + Fe) ratio increases with increasing degree of oxidation of the host rocks. Bard (1970) has found a similar relation in the Ca-amphiboles from a comparable geologic setting in Spain.

TiO_2 content of the amphiboles is variable. It does not increase with the prograde metamorphism as has been found at higher grades by other authors (Binns, 1965b; Engel and Engel, 1962); rather it seems to depend on the available TiO_2 content of the host rocks. It is lowest in amphiboles from meta-gabbro 796 in which percentage of TiO_2 is only 0.11 (Hietanen, 1973). It is highest in amphiboles from the low grade meta-andesite (sample 463) and metadiorite (sample 465) that have 0.75 and 0.54

percent TiO_2, originally contained in sphene and pyroxene. Metabasalt sample 551 has 2.03 percent TiO_2, but most of it is in ilmenite that was more stable than sphene and pyroxene during recrystallization.

Influence of Temperature

The composition of the aluminous hornblende is influenced more by the grade of metamorphism than is the composition of actinolite. Comparison of amphiboles from metagabbro (sample 796), collected 0.3 mile from the pluton, and those from metabasalt (sample 551), 0.8 mile from the pluton, reveals that those closer to the pluton (sample 796) contain blue-green hornblende that is richer in Al^{iv} and alkalies than hornblendes from those farther from the pluton. Thin-section studies of scores of other specimens show that generally near the contacts of the plutons the hornblende is blue green, whereas elsewhere the amphiboles are green to pale green. Analyzed green hornblendes such as those in metadiorite samples 465 and 532 contain much less aluminum and alkalies but have about the same iron-magnesium ratio as the blue-green hornblende in sample 796 (1-3, Table 2b). Thus the Al^{iv} and alkali contents of the hornblende increase with increasing grade of metamorphism, whereas the iron-magnesium ratio depends on the bulk composition of the host rock.

Increase in the alkali and Al^{iv} contents of hornblende with increasing grade of metamorphism has been reported by many earlier workers in different parts of the world (e.g., Deer, Howie, and Zussman, 1963, pp. 304-305). Binns (1965a, b) found a prograde increase in the content of alkalies, titanium, and tetrahedral aluminum in hornblendes from basic hornfelses at Tilbuster and in the Broken Hill district, New South Wales. However, in a similar contact zone at Moonbi, the content of Al^{iv} in hornblende remained roughly constant. Cahill (*nee* Macara, 1968) described a definite increase in Al^{iv} and alkali contents in hornblendes from basic hornfelses in southern New South Wales. Bard (1970) has pointed out that an enrichment of alkalies and increase in Ti and Al^{iv} contents in hornblende with the increasing P and T exists but that their extent varies.

The relation between the tetrahedral Al contents of the amphibole pairs—actinolite and hornblende—and the estimated temperature of recrystallization in the Feather River area is shown graphically in
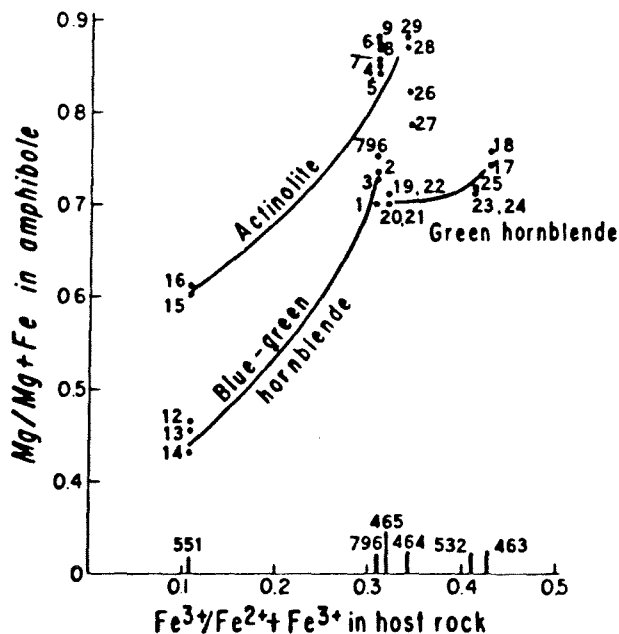

FIG. 6. Plot of Mg/(Fe + Mg) in the amphiboles against $Fe^{3+}/(Fe^{2+} + Fe^{3+})$ in the analyzed host rocks. Numbers along abscissa refer to rock analyses in Hietanen (1973).

Figure 7. The temperature in the zone next to the contact (Fig. 1, sample 796, 546) of the plutons is estimated at 600°C on the basis of absence of sillimanite and coexistence of andalusite and cordierite in the pelitic layers. In the zone 0.6 to 1.2 miles from the contact (sample 551 and 532), where staurolite occurs with andalusite in the pelitic layers, temperature may have been about 500°C. For samples 465, 463, and 464 that are 3.2 miles from the contact, the temperature of recrystallization was estimated at 350°C on the basis of mineral assemblages albite-actinolite-clinozoisite-epidote-chlorite and albite-chlorite-muscovite-biotite without garnet. Two curves connecting the actinolites on one hand and the aluminous amphiboles on the other were drawn by visual inspection. The points for the amphibole in sample 532 (23, 24, 25) fall in the "miscibility gap" between actinolites and hornblendes of medium temperature. This quartz diorite has only one amphibole and only one epidote mineral, suggesting that it crystallized in physical conditions that were different from those of the other specimens in this zone. It may be a later dike crystallized at igneous temperatures as shown by arrows in Figure 7. The tetrahedral Al content in the "igneous" hornblende in this area (Hietanen, 1971) is plotted in Figure 7 (474, 522) at temperatures of the beginning of the melting of quartz diorite and quartz monzonite in order to indicate the upper limit of the possible immiscibility.

The coexistence of two amphiboles, actinolite and aluminous hornblende, has been previously described by Shido (1958) and by Shido and Miyashiro (1959) from the Abukuma plateau, Japan, and from two specimens of epidiorite in the Scottish Highlands. According to their descriptions, the parallel intergrowths and patches and rims of blue-green hornblende within and around actinolite are similar to the intergrowths of actinolite and aluminous hornblende in the Feather River area. Shido and Miyashiro (1959) suggested that there may be a miscibility gap between the actinolite and hornblende at about 1.0 Al^{iv}. The Al^{iv} content, however, is typical of the green hornblende in the Feather River area, and the miscibility gap, if any, is a function of T (Fig. 7). Also Klein (1969) suggested that coexisting amphiboles may very likely represent equilibrium pairs across a miscibility gap.

Epidote Minerals

Electron-microprobe analyses of epidote minerals (Table 3) represent relatively homogeneous single
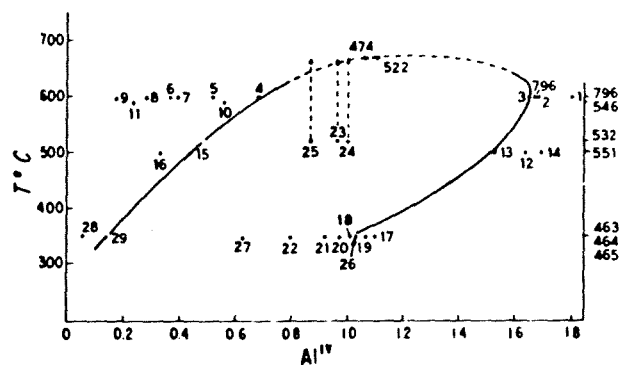

FIG. 7. Estimated temperature of recrystallization of the amphiboles against tetrahedral Al per 23(O). Numbers refer to Table 2. Points (X) are for "igneous" hornblende from Hietanen (1971).

grains or groups of grains; exceptions are discussed below. Composition ranges from zoisite and clinozoisite with little iron to epidotes with pistacite, $Ca_2Fe^{3+}_3$ $Si_3O_{12}(OH)$, contents as much as 26 molecular percent. Most analyses show small amounts of manganese, titanium, and potassium. In the calculated formula units, the silicon content is only a little higher than the ideal three atoms, and the calcium content is somewhat lower than two atoms. Two analyses (30 and 31) of zoisite in metagabbro sample 796 have some sodium that replaces calcium. The variation of Al and total Fe as Fe^{3+} is shown in Figure 8. All analyses except 38 fall on a linear trend as they should. Analysis 38 was computed using the two highest iron counts from the grain; the remainder of the counts gives analysis 36. Analysis 38 is thus not an independent analysis but rather shows, together with analysis 36, the extent of possible variation in iron content within an individual grain. Analysis 37 from the same specimen represents a homogeneous
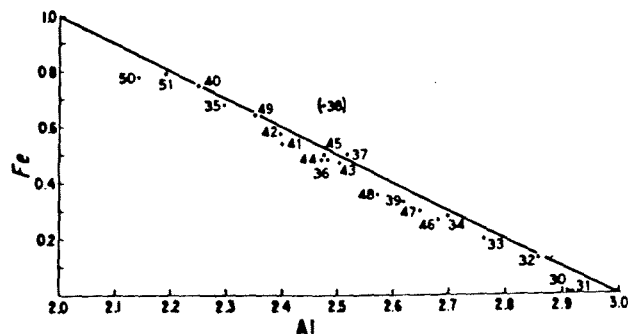

FIG. 8. Plot of Fe^{3+} against Al in the epidote minerals. Numbers refer to Table 3.

grain; thus 36 and 37 indicate the dominant composition.

The range of pistacite content in some individual samples is greater, and in others smaller, than would be expected on the basis of the indices of refraction measured on the mineral powders. Some of this discrepancy results from averaging the counts in the microprobe analyses. For instance, analyses of epidote in sample 465 (Table 3, anal. 41 and 42) show 18 to 19 percent iron end member (pistacite), but the highest microprobe counts for iron in this sample correspond to 11 percent FeO, equivalent to 22 molecular percent pistacite. In contrast, the lowest counts yield 6 percent FeO and thus about 12 molecular percent pistacite. Both clinozoisite and epidote were identified optically in mineral powder (Table 1). The composition based on the high iron counts is in agreement with the highest indices of refraction measured, but the lowest counts correspond to a higher content of pistacite than is indicated by the lowest indices of refraction. These relations are in general agreement with the exsolution textures seen in immersed grains (Fig. 3). Further discrepancies result from the inhomogeneity of the host rocks; the probe analyses were made in a single polished thin section, which represents a limited sampling of the specimen from which mineral concentrate for immersion work was prepared. For example, in sample 532 high index domains ($\gamma = 1.754$, Ps 22) were determined optically in some grains of bulk composition Ps 14 ($\gamma = 1.742$). The electron-microprobe data for epidote in this sample (Table 3, anal. 43–45), however, indicate that the analyzed grains are homogeneous and contain 16 to 17 percent pistacite. Only two of the three epidote minerals in the metagabbro sample 796 were present in the polished thin section; the third is an epidote optically similar to epidote in samples 532 and 551. Clinozoisite in sample 796 is inhomogeneous; analyses 31 and 34, representing discrete crystals, reflect the observed limits in Ps content. Zoisite in sample 796 occurs as veinlets and pods and formed later than the other epidote minerals.

Thus the results of electron microprobe work and the indices of refraction together with exsolution textures suggest that two distinct phases, an iron-poor clinozoisite and iron-rich epidote, are present in all samples except in sample 532. A similar relationship has been discussed by Strens (1965) from two localities where a "miscibility gap" in the clinozoisite-epidote series occurred between compositions

Ps 8 and Ps 28 at low temperatures. Sterns attributed this to the presence of strain in the mixed crystals at temperatures below 550°C.

This can be further considered in the light of the structure of epidote. According to Ito, Morimoto, and Sadanaga (1954), epidote consists of chains of $(Al,Fe^{3+})O_6$ and $(Al,Fe^{3+})O_4(OH)_2$ octahedra parallel to b axis and bound together by Al,Fe^{3+}, Ca, and Si atoms. Miyashiro and Seki (1958) have suggested that the AlO and AlOH sites in the chains are filled mainly with Al atoms whereas the Fe^{3+} atoms are located between the chains. In the common epidote $Ca_2Al_2FeSi_3O_{12}(OH)$ all the octahedral sites between the chains would be occupied by Fe^{3+} to give a "stable" or unstrained structure.

According to the recent refinement of epidote structure by Dollase (1971), the edge-sharing Al octahedra form two types of chains: a single chain of $M(2)$ octahedra and a multiple zig-zag chain of central $M(1)$ and peripheral $M(3)$. These chains are cross-linked by SiO_4 and Si_2O_7 groups and Ca is in large cavities between the chains and links. The single chain octahedra $M(2)$ contain only Al atoms and the substitution in the multiple $M(1)$-$M(3)$ chain is nonuniform, the $M(3)$ sites containing a larger fraction of Fe^{3+} than the $M(1)$ site. In the low-iron epidote, all Fe^{3+} is in $M(3)$ sites.

All the analyzed epidotes (Table 3) have considerably more Al than would be necessary to fill the $M(2)$ and $M(1)$ sites in chains. If it is assumed that all Fe^{3+} is in $M(3)$ sites, about 3/4 of these sites are filled with Fe^{3+} in epidotes from the low grade zone and only about 1/3 of these sites in the coexisting clinozoisite contain Fe^{3+}. In epidotes from the high grade zone (Sp. 551, 546), about 1/2 of the $M(3)$ sites are occupied by Fe^{3+} atoms. These differences in the extent of substitution of Fe^{3+} for Al indicate that certain substitutions may be more stable than some others at a given temperature.

Myer (1966) has reported coexistence of ferrian zoisite and epidote from calc-silicate rocks in Norway. Compositions given by him indicate 0.11 Fe^{3+} atoms per formula unit in ferrian zoisite ($Ca_2Al_{2.89}Fe^{3+}_{0.11}Si_3O_{12}OH$) and 0.37 to 0.63 Fe^{3+} atoms in coexisting epidote $Ca_2(Al,Fe^{3+})_3Si_3O_{12}OH$.

The stability relations between the epidote minerals have been experimentally investigated by Nitsch and Winkler (1965) and by Holdaway (1966). According to Holdaway (1966), clinozoisite and quartz react to form anorthite plus grossularite at about 660°C at pressure of 4 kbar. Nearly similar

results were obtained by Nitsch and Winkler (1965), who further showed that at pressures higher than 3.5 kbar the stability field of zoisite extends to a higher temperature than that of epidote. This relation may explain the occurrence of zoisite near the contact of Granite Basin pluton (sample 796). At elevated temperatures near the pluton, zoisite crystallized in addition to clinozoisite.

Chlorite and Muscovite

The composition of chlorite (Table 4) is more uniform than that of the amphiboles and epidote minerals. Tetrahedral Al is close to 2.5, and octahedral Al is 2.55 to 2.73 in all analyzed chlorites. Mg/(Fe + Mg) ratio is 0.64 to 0.83, and the chlorite in metagabbro sample 796 is richest in aluminum and magnesium.

Some muscovite occurs with chlorite in metagabbro sample 796. Electron-microprobe analysis (Table 4) shows that it is a potassium-aluminum mica with only about 1 percent MgO and little sodium and iron. Its phengite content is about 7 molecular percent.

Plagioclase

Plagioclase is anorthite in metagabbro sample 796 and bytownite (An$_{71}$) in the metagabbro sample 546 (Tables 1 and 5). In all the other specimens, it is albite. The presence of irregular twinning lamellae with relict granular textures in specimen 796 suggests that the anorthite crystallized from zoisite at elevated temperatures. This unusual sequence of crystallization is supported by the extreme composition of anorthitic plagioclase. The bulk composition of the host rocks (Hietanen, 1973) indicates extensive changes in the chemistry of all metavolcanic and meta-igneous rocks during their recrystallization. All are impoverished in potassium, and most also in sodium. As a result, petrochemical norm calculations yield a high anorthite content for plagioclase. Anorthitic plagioclase crystallized in equilibrium with epidote from this composition at temperatures close to 600°C.

Distribution of Fe, Mg, and Al Among Hornblende, Chlorite, and Epidote

The occurrence of amphibole pairs and two to three epidote minerals together raises the question of distribution of elements among these minerals. It is evident that the distribution changes with the increase in metamorphic temperatures. Normally,

iron-rich epidote crystallizes with magnesian actinolite at low temperatures of the green schist facies. Clinozoisite and epidote are common with hornblende at intermediate temperatures whereas zoisite is the only epidote mineral at very high temperatures and pressures. Since the major changes in composition in both mineral groups are tied to the changes in Al and Fe contents, the percentages of Al$_2$O$_3$ and FeO for each mineral in samples from the high grade zone were plotted in the same graph (Fig. 9). Individual analysis points for each mineral were connected by a solid line, which shows the range of Al$_2$O$_3$ and FeO contents.
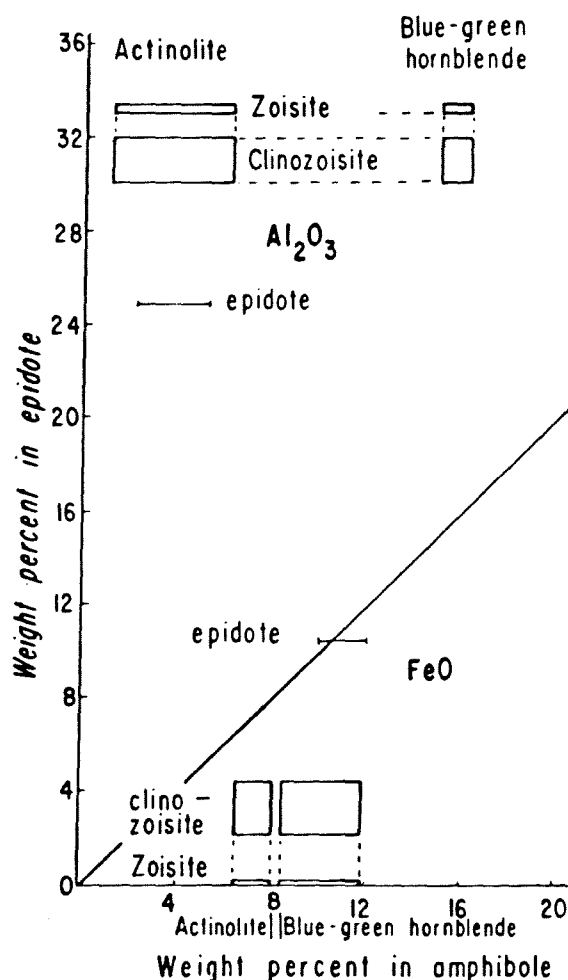

FIG. 9. Distribution of Al$_2$O$_3$ and FeO in the analyzed amphiboles and epidote minerals in the high grade zone. The range of the percentage of these oxides in minerals is shown by solid lines, and the coexisting minerals of the same species in sample 796 are connected with broken lines. Epidote is from sample 546; optically similar epidote coexists with the other minerals in sample 796. Line OA shows the equal distribution.

In the upper half of Figure 9, the abscissa shows the range in Al_2O_3 percentages in amphiboles, and the ordinate shows the range in Al_2O_3 percentages in epidotes. For easier observance, the actinolite-hornblende pairs and the zoisite-clinozoisite pairs in sample 796 were connected with broken lines. A gap in the Al_2O_3 content between the actinolite and bluegreen hornblende at the highest grade is wide in spite of the overlap of the Al_2O_3 percentage in this actinolite and in the green hornblende. In contrast, the gap in the FeO content (lower part in Fig. 9) is small; all the actinolites, however, have a lower FeO content than the hornblende. Most samples from the low grade zone contain actinolite + green hornblende, but in samples 463, 465, and 532 only the medium-Al hornblende was present in the polished thin section.

Only a small gap exists in the Al_2O_3 and FeO contents between the coexisting zoisite and clinozoisite, whereas epidote contains much less Al_2O_3 and more FeO than the coexisting clinozoisite. The gap between the clinozoisite and epidote in the low grade zone is distinct in samples 464 and 463, but in sample 465 only an intermediate composition occurs. This intermediate composition, however, includes inhomogeneous counts, which, if separated, would give composition similar to the clinozoisite and epidote in the other samples.

The Fe/Al ratio is large in the low-Al actinolites and decreases rapidly with increasing Al content. In actinolitic hornblende this ratio is 1.6, in green hornblende 1.1 to 1.3, and in the blue-green hornblende at the highest grade it is 0.5. In the blue-green hornblende in metabasalt (sample 551), which is rich in Fe, the Fe/Al is of the same magnitude as in the green hornblende even if this sample comes from a higher grade zone. This shows that Fe/Al ratio generally decreases with increasing temperature but is also influenced by the Fe/Al ratio of the host rock.

Comparison of the average Fe/Al ratios in the coexisting epidote and clinozoisite from the low-grade zone (0.33 and 0.13 respectively; Sp. 463 and 464) with those from the high-grade zone (0.28 and 0.2, Sp. 551 and 546) suggests that the difference between the Fe/Al values of the coexisting epidote minerals is smaller in the high-grade zone. Epidote from the highest grade zone (sample 796) was not analyzed because none was found in the polished thin section. The indices of refraction measured in the mineral powder, however, suggest that epidote in this rock is very similar in composition to that in

sample 551. Using the Fe/Al ratio of this epidote (0.27, Sp. 551), the distribution coefficient K_D(Fe/Al) for epidote/clinozoisite in the highest grade zone is calculated as $K_D = 2.9$, thus somewhat larger than the corresponding value in the low grade zone ($K_D = 2.6$) and much larger than $K_D = 1.6$ in sample 551. This reversal of trend is due to a low content of iron in clinozoisite (Sp. 796) that has rims of zoisite dusted by iron oxide. Probably a part of the iron originally present in this clinozoisite was exsolved upon the beginning of its transformation to zoisite.

All chlorites are rich in aluminum, but the magnesium/iron ratio ranges from 1.7 to 4.4, the chlorite in sample 796 being richest in magnesium. Distribution coefficients are different for amphiboles with different Al contents, as shown in Figure 10. For the hornblendes of median Al content (464h, 463h, 465h), K_D(Mg/Fe) chlorite/hornblende is generally between 0.7 and 1.2, and there is no observable change with the temperature of metamorphism (comp. 546h). However, the chlorite in the zone next to the pluton (in metagabbro Sp. 796) is richer in magnesium and contains less iron than any other chlorite. K_D(Mg/Fe) (chlorite/hornblende) in this rock is 1.9, more than twice that for the chlorite and the average median-Al hornblende in the low grade rocks.

Summary and Conclusions

In the outer contact aureoles of the Cretaceous plutons, Northern Sierra Nevada, where the mineral assemblages indicate PT conditions at the border of the greenschist and epidote amphibole facies, green hornblende occurs with actinolite, chlorite, clinozoisite, epidote, and albite. In the zone next to the plutons, where the occurrence of andalusite with cordierite and prograde pseudomorphs of muscovite after staurolite in interlayered pelitic rocks indicates PT conditions at the higher limit of the epidote amphibolite facies ($T \sim 650°C$ at $P \sim 4$ kbar), hornblende is blue green, and plagioclase is rich in the anorthite molecule. Zoisite occurs with other epidote minerals.

The electron-microprobe analyses show that the alkali and aluminum contents of the hornblende increase with increasing grade of metamorphism, but their ratio remains constant. The generalized structural formula of the green hornblende is $(Na,K)_{0.3}$ $Ca_2(Mg,Fe^{2+})_{4.4}(Al,Fe^{3+},Ti)_{0.6}AlSi_7O_{22}(OH)_2$ and that of the blue-green hornblende is $(Na,K)_{0.5}Ca_2$

$(Mg,Fe)_{3.6}(Al,Fe^{3+})_{1.2}Al_{1.7}Si_{6.3}O_{22}(OH)_2$. The ratio of $(Na + K)^A/Al^{iv}$ remains close to 0.3. The end member in this actinolite-hornblende series is the hornblende $(Na,K)_{0.6}Ca_2(Mg,Fe)_{3.6}(Al,Fe^{3+})_{1.4}Al_2$ $Si_6O_{22}(OH)_2$, which is derived from the actinolite by two coupled substitutions—edenitic ($NaAl^{iv}$ for $\square^A$ Si^{iv}) and tschermakitic ($Al^{vi}Al^{iv}$ for $Mg^{vi}Si^{iv}$) at the ratio of 3:7.

The $Mg/(Mg + Fe)$ ratio in amphiboles depends on the bulk composition and the degree of oxidation of the host rocks. The Ti content of hornblende reflects the amount of available Ti in the host rocks.

The coexistence of two Ca amphiboles implies the existence of a miscibility gap, if the amphiboles crystallized in equilibrium. The composition of hornblende in the border zone of the plutonic rocks provides the upper limit of the possible immiscibility.

Two epidote minerals—clinozoisite and epidote with pistacite content from 10 to 26 percent—coexist with actinolite, hornblende, chlorite, and plagioclase in all zones. Zoisite with anorthitic plagioclase crystallized at the highest grade. Elsewhere plagioclase is albite. The miscibility gap of epidote and clinozoisite at temperatures below 600°C is suggested by compositions of the coexisting mineral pairs.

The Fe/Al ratio in epidote decreases slightly with increase in the grade of metamorphism, whereas in hornblende the decrease in this ratio is much greater; Fe/Al in the high grade hornblende is one half of that in the low grade hornblende. There is no regular change in $K_D(Fe/Mg)$ for chlorite/hornblende, al-

though it is highest in the zone next to the plutons. It seems reasonable to assume that pressure remained approximately at the same level during the metamorphism and that the changes described are due to the elevated temperatures near the plutons.

References

BARD, J. P. (1970) Composition of hornblendes formed during the Hercynian progressive metamorphism of the Aracene Metamorphic Belt (SW Spain). *Contrib. Mineral. Petrology*, **28**, 117–134.

BEESON, M. H. (1967) A computer program for processing electron microprobe data. *U.S. Geol. Surv. Open-File Rep.*, 10 pp.

BINNS, R. A. (1965a) Hornblendes from some basic hornfelses in the New England region, New South Wales. *Mineral. Mag.* **34**, 52-65.

—— (1965b) The mineralogy of metamorphosed basic rocks from the Willyama Complex, Broken Hill district, New South Wales. Part 1. Hornblendes. *Mineral. Mag.* **35**, 306–326.

CAHILL (*nee* MACARA), B. J. (1968) The use of amphiboles to illustrate trends in contact metamorphism. *IMA 5th Gen. Meet. Cambridge 1966*, 189–203.

COMPTON, R. R. (1958) Significance of amphibole paragenesis in the Bidwell Bar region, California. *Amer. Mineral.* **43**, 890–907.

DEER, W. A., R. A. HOWIE, AND J. ZUSSMAN (1963) *Rock Forming Minerals*, Vol. 2. *Chain Silicates*. Longmans, Green and Co., Ltd., London, 379 pp.

DESBOROUGH, G. A., AND R. H. HEIDEL (1971) Improved electron microprobe analysis at low operating voltage. 1. Silicon, magnesium and aluminum. *Amer. Mineral.* **56**, 2129–2135.

DOLLASE, W. A. (1971) Refinement of the crystal structures of epidote, allanite, and hancockite. *Amer. Mineral.* **56**, 477–464.

ENGEL, A. E. J., AND C. G. ENGEL (1962) Hornblendes formed during progressive metamorphism of amphibolites, northwest Adirondack Mountains, New York, *Geol. Soc. Amer. Bull.* **73**, 1499–1514.

ERNST, W. G. (1968) *Amphiboles*. Vol. 1, *Minerals, Rocks, and Inorganic Materials*. Springer-Verlag, Inc., New York. 125 pp.

FREY, MARTIN (1969) Die Metamorphose des Keupers vom Tafeljura bis zum Lukmanier-Gebiet. *Beitr. Geol. Karte Schweiz*, **137**, 1–160.

GOLDICH, S. S., C. O. INGAMELLS, N. H. SUHR, AND D. H. ANDERSON (1967) Analyses of silicate rock and mineral standards. *Can. J. Earth Sci.* **4**, 747–755.

HAFNER, STEFAN (1958) Petrographie des südwestlichen Gotthardmassivs (zwischen St.-Gotthardpass und Nufenenpass). *Schweiz. Mineral. Petrogr. Mitt.*, **38**, 255–362.

HEZNER, L. (1909) Petrographische Untersuchung der kristallinen Schiefer auf der Südseite des St. Gotthard (Tremolaserie). *Neues Jahrb. Mineral. Geol. Pal.* B.-B **27**, 157–218.

HIETANEN, ANNA (1951) Metamorphic and igneous rocks of the Merrimac area, Plumas National Forest, California. *Geol. Soc. Amer. Bull.* **62**, 565–608.
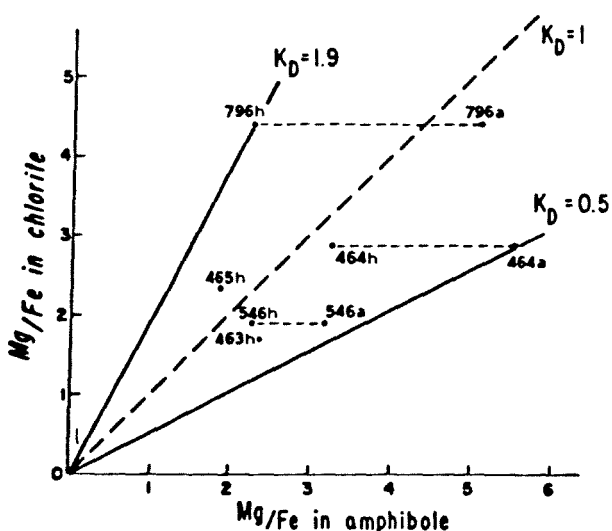
FIG. 10. Distribution coefficient for average of Mg/Fe in coexisting chlorite and actinolite (a) and chlorite and hornblende (h). The numbers refer to the host rock samples.

—— (1959) Kyanite-garnet gedritite near Orofino, Idaho. *Amer. Mineral.* **44,** 539–564.

—— (1963) Anorthosite and associated rocks in the Boehls Butte quadrangle and vicinity, Idaho. *U.S. Geol. Surv. Prof. Pap.* **344-B,** 78 pp.

—— (1967) On the facies series in various types of metamorphism. *J. Geol.* **175,** 187–214.

—— (1971) Distribution of elements in biotite-hornblende pairs and in an orthopyroxene-clinopyroxene pair from zoned plutons, northern Sierra Nevada, California. *Contrib. Mineral. Petrology,* **30,** 161–176.

—— (1973) Geology of the Pulga and Bucks Lake quadrangles, Butte and Plumas Counties, California. *U.S. Geol. Surv. Prof. Pap.* **731.**

HOLDAWAY, M. J. (1966) Hydrothermal stability of clinozoisite plus quartz. *Amer. J. Sci.* **264,** 643–667.

ITO, T., N. MORIMOTO, AND R. SADANAGA (1954) On the structure of epidote. *Acta Crystallogr.* **7,** 53–59.

KLEIN, CORNELIS, JR. (1969) Two-amphibole assemblages in the system actinolite-hornblende-glaucophane. *Am. Mineral.* **54,** 212–237.

LEAKE, B. E. (1965a) The relationship between composition of calciferous amphibole and grade of metamorphism. In *Controls of Metamorphism,* W. S. Pitcher and G. W. Flinn, Eds, John Wiley and Sons, Inc., New York, pp. 299–318.

—— (1965b) The relationship between tetrahedral aluminum and the maximum possible octahedral aluminum in natural calciferous and subcalciferous amphiboles. *Amer. Mineral.* **50,** 843–851.

—— (1968) A catalog of analysed calciferous and subcalciferous amphiboles together with their nomenclature and associated minerals. *Geol. Soc. Amer. Spec. Pap.* **98,** 210 pp.

—— (1971) On aluminous and edenitic hornblendes. *Mineral. Mag.* **38,** 389–407.

MIYASHIRO, A., AND Y. SEKI, (1958) Enlargement of the composition field of epidote and piemontite and rising temperature. *Amer. J. Sci.* **256,** 423–430.

MYER, G. H. (1966) New data on zoisite and epidote. *Amer. J. Sci.* **264,** 364–385.

NITSCH, K. H., AND H. G. F. WINKLER, (1965) Bildungsbedingungen von Epidot und Orthozoisit. *Beitr. Mineral. Petrology,* **11,** 470–486.

PAPIKE, J. J., MALCOLM ROSS, AND JOAN R. CLARK (1969) Crystal-chemical characterization of clino-amphiboles based on five new structure refinements. *Mineral. Soc. Amer. Spec. Pap.* **2,** 117–136.

PHILLIPS, R., AND W. LAYTON (1964) The calciferous and alkali amphiboles. *Mineral. Mag.* **33,** 1097–1109.

ROBINSON, P., M. ROSS, AND H. W. JAFFE (1971) Composition of the anthophyllite-gedrite series, comparisons of gedrite and hornblende, and the anthophyllite-gedrite solvus. *Amer. Mineral.* **56,** 1005–1041.

SHIDO, F. (1958) Plutonic and metamorphic rocks of the Nakoso and Iritono districts in the central Abukuma Plateau. *J. Fac. Sci, Univ. Tokyo, Sec. 2,* **11,** *Pt.* **2,** 131–217.

——, AND A. MYASHIRO (1959) Hornblendes of basic metamorphic rocks. *J. Fac. Sci., Univ. Tokyo, Sec. 2,* **12,** *Pt.* **1,** 85–102.

STEIGER, RUDOLF (1961) Die hornblende der Tremolaseries. Teil 1. Chemismus and Dichte der Hornblenden. *Schweiz. Mineral. Petrogr. Mitt.* **41,** 127–156.

STRENS, R. G. J. (1965) Stability relations of the Al-Fe epidotes. *Mineral Mag.* **35,** 464–475.